Tunability and enhancement of mechanical behavior with additively manufactured bio-inspired hierarchical suture interfaces

Erica Lin
Department of Materials Science and Engineering, Massachusetts Institute of Technology, Cambridge, MA 02139, USA

Yaning Li
Department of Mechanical Engineering, University of New Hampshire, Durham, NH 03824, USA

James C. Weaver
Wyss Institute for Biologically Inspired Engineering, Harvard University, Cambridge, MA 02138, USA

Christine Ortiz
Department of Materials Science and Engineering, Massachusetts Institute of Technology, Cambridge, MA 02139, USA

Mary C. Boyce[a)]
Department of Mechanical Engineering, Massachusetts Institute of Technology, Cambridge, MA 02139, USA; and School of Engineering and Applied Sciences, Columbia University, New York, NY 10027, USA

(Received 8 April 2014; accepted 20 June 2014)

In nature, biological structures often exhibit complex geometries that serve a wide range of specific mechanical functions. One such example are the ammonites, a large group of extinct mollusks, which produced elaborate, fractal-like hierarchical suture interface patterns. This report experimentally explores the influence of hierarchical suture interface designs on mechanical behavior by taking advantage of additive manufacturing and its ability to fabricate complex geometries. In addition, structure/property relationships of additively manufactured multi-material prototypes are investigated. It is shown that increasing the order of hierarchy amplifies stiffness by more than an order of magnitude. Tensile strength can also be tailored by changing the order of hierarchy, which alters the normal to shear stress ratio of the interfacial layer. The addition of failure mechanisms with increased order of hierarchy also significantly increases the toughness. Therefore, hierarchical suture interfaces can be used to diversify the mechanical behavior of additively manufactured materials.

I. INTRODUCTION

Additive manufacturing, with its ability to rapidly fabricate complex geometries, has emerged as a useful approach for prototyping and understanding the mechanical behavior of new material designs.[1–4] Materials in nature often possess complex geometries that are critical for their mechanical performance,[5–7] and therefore the use of additive manufacturing for prototyping bio-inspired materials designs is a particularly powerful experimental research platform. These complex geometries are often hierarchical, both across[8,9] and within[10,11] length scales. Hierarchical designs within a given length scale consist of intricate, fractal-like patterns with repeating self-similar geometries, and have been shown to contribute significantly to the mechanical properties of natural materials.[12,13]

One particularly fascinating example of hierarchical design in nature is suture interfaces, which consist of interdigitating stiffer components, or teeth, joined by a compliant interfacial layer.[11,12,14–17] Suture interface geometries vary significantly both across species, ranging from the triangular waveform of the three-spined stickleback[18] to the intricate, hierarchical designs of ammonites.[19,20] As shown in Fig. 1(a), even within ammonites, suture interfaces exhibit various geometries, from simple curves to complex, hierarchical geometries.[11,21,22]

We have recently shown through analytical models that simple changes in first-order geometries and frequency of suture interfaces without any hierarchical designs can finely tune the stiffness, strength, toughness, and failure mechanisms of the overall structure.[17,23] In addition, we have shown through analytical models that the hierarchical design of suture interfaces can be used to tailor and amplify mechanical properties nonlinearly.[20] Here, we further explore the role of hierarchy in mechanical behavior through direct mechanical testing on additively manufactured prototypes. Through the use of prototyping by 3D-printing, not only can the influence of hierarchical geometry on mechanical behavior, including stiffness,

[a)]Address all correspondence to this author.
e-mail: mcboyce@mit.edu
DOI: 10.1557/jmr.2014.175

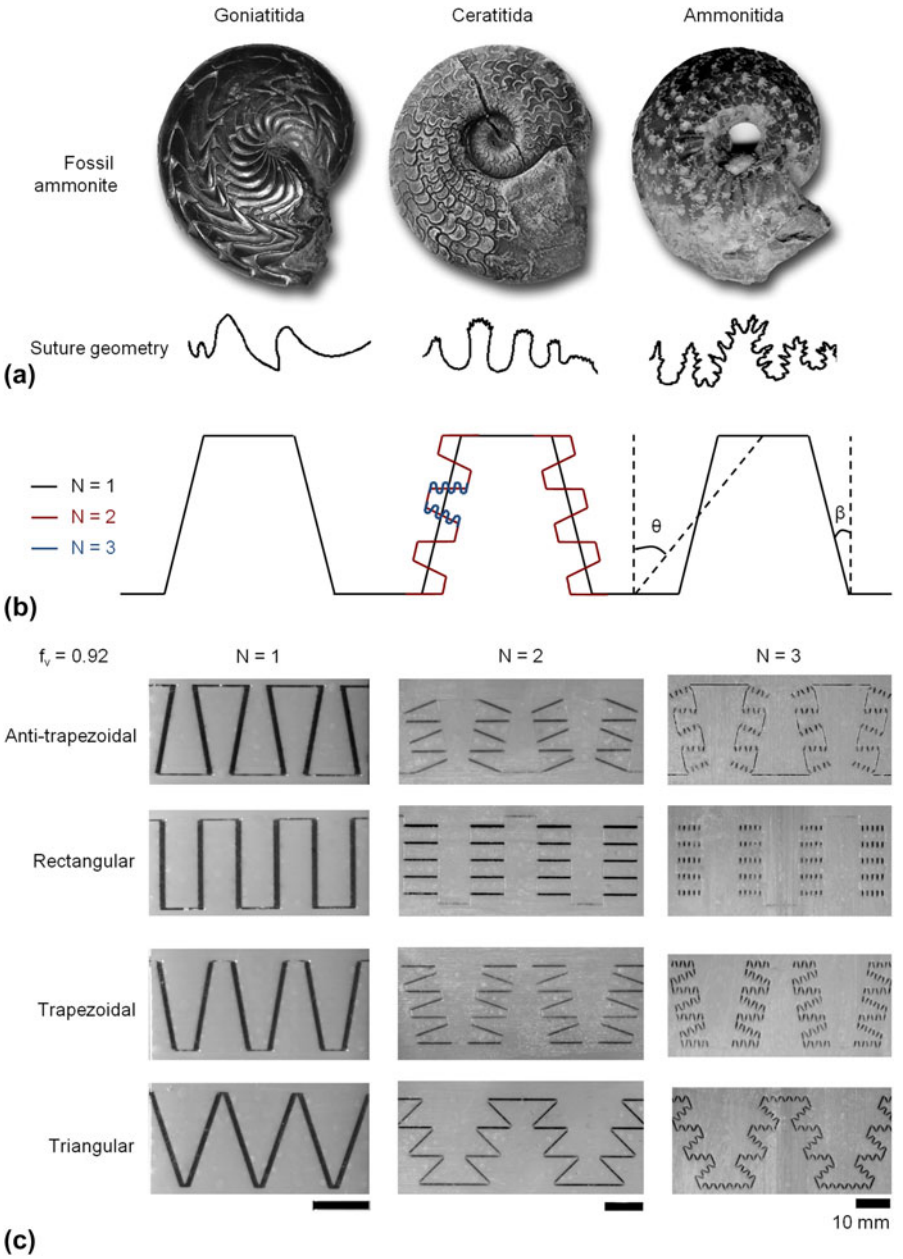

FIG. 1. Ammonite-inspired design of hierarchical suture interfaces. (a) Photographs illustrating the progressive increase in ammonite suture structural complexity, (b) schematic of hierarchical suture interface design, (c) optical images of 3D-printed prototypes of anti-trapezoidal, rectangular, trapezoidal, and triangular suture interfaces with $N = 1$, 2, and 3 at a volume fraction, f_v, of 92%. (Images in (a) adapted from Wikimedia Commons).

strength, and toughness be experimentally determined, but also the failure mechanisms and post-failure behavior can be investigated. In addition, through direct mechanical testing of 3D-printed prototypes, the mechanical behavior of additively manufactured materials can be further explored and understood.

In this paper, we experimentally investigate the stiffness, strength, toughness, and failure mechanisms of hierarchical suture interfaces by utilizing additive manufacturing to create physical prototypes. Bio-inspired design principles are extracted and hierarchical designs are explored as a method of expanding the range of mechanical behaviors that additively manufactured materials possess. Through this study, a deeper understanding of structure/property relationships of geometrically structured, multi-material, additively manufactured prototypes is also elucidated.

II. METHODS

Hierarchical suture interfaces with four geometries (anti-trapezoidal, rectangular, trapezoidal, and triangular) and three orders of hierarchy ($N = 1$, 2, and 3) were

designed. The four geometries were general trapezoidal geometries introduced in Li et al. (2012), that are defined by the relationship between the shape factor, β, and tip angle, θ, shown in Fig. 1(a): anti-trapezoidal if $-\theta < \beta < 0$, rectangular if $\beta = 0$, trapezoidal if $0 < \beta < \theta$, triangular if $\beta = \theta$. All fabricated suture interface designs have $\theta = 21.8°$, and $\beta = -\theta/2$ and $\beta = \theta/2$ for anti-trapezoidal and trapezoidal geometries, respectively. Higher order hierarchical designs were created by iteratively superimposing self-similar waveforms on the slant interfaces of former suture interface profiles, as shown in Fig. 1(a). A tooth volume fraction, f_v, of 92% and an interface width of 0.5 mm were maintained for all designs. The major teeth were defined as the teeth of the first-order suture interface profile, while the minor teeth were defined as the teeth corresponding to higher order suture interface profiles.

The hierarchical suture interface prototypes were designed within Solidworks (Dassault Systemes, 2013) and fabricated via multi-material additive manufacturing (Stratasys Ltd., Eden Prairie, MN) as shown in Fig. 1(b). VeroWhite, an acrylic-based photo-polymer, was utilized for the teeth, and TangoPlus, a rubber-like compliant material, was used for the interfacial layer. The Young's moduli of TangoPlus (E_0) and VeroWhite (E_1) were previously determined to be 0.63 ± 0.02 MPa and 2.0 ± 0.09 GPa, respectively. In addition, the tensile and shear strength were previously determined to be 1.8 ± 0.94 MPa and 1.4 ± 0.11 MPa, respectively, for an interfacial layer of 0.5 mm.[24] These material properties were used for the analytical predictions of the various suture interfaces and primary failure modes were found to be cohesive failures within the interfacial layer.

Three samples of each geometry were mechanically tested with a Zwick mechanical tester (Zwick Z010, Zwick Roell, Germany) under longitudinal tension at a constant strain rate of 0.05 s^{-1} for force–displacement measurements. Speckle patterns were created with an airbrush and a video extensometer in conjunction with digital image correlation (DIC) software: VIC-2D (Correlated Solutions, Inc., 2009) was used to calculate the local strain in the suture area. After mechanical testing, the fractured samples were sputter coated with gold and examined by scanning electron microscopy (SEM).

III. RESULTS

The different geometries and orders of hierarchy (N) resulted in a wide range of mechanical behaviors as seen in Fig. 2. In this paper, we focused on the stiffness, strength, toughness, and failure mechanisms of the hierarchical suture interfaces under longitudinal tension. In the following section, the influence of the order of hierarchy on the mechanical behavior of suture interfaces with different geometries are discussed in detail.

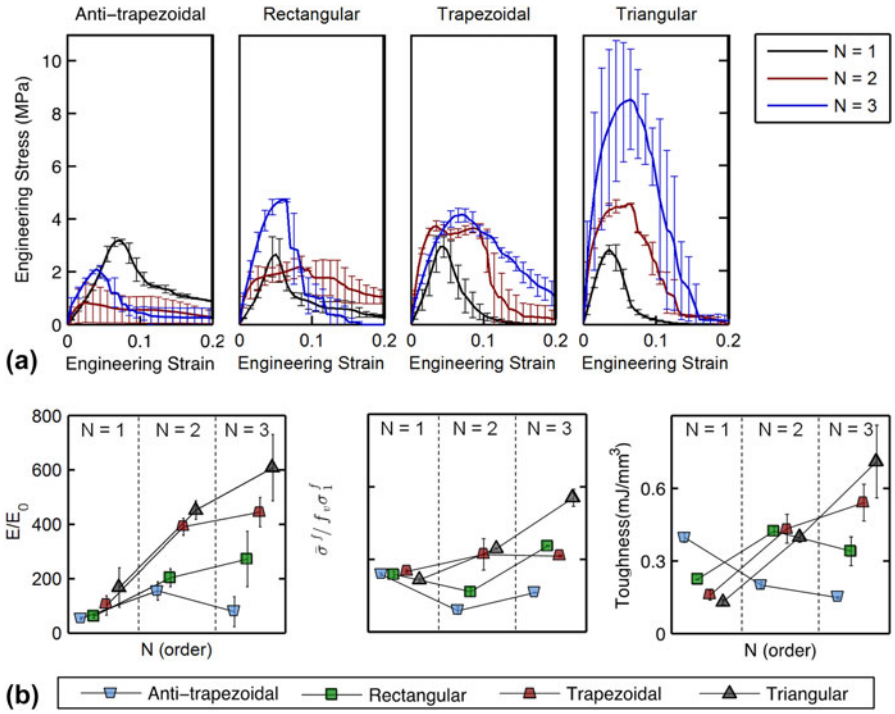

FIG. 2. Mechanical behavior of hierarchical suture interfaces under longitudinal tension. (a) Engineering stress–strain curves of hierarchical suture interfaces, (b) non-dimensional effective stiffness and strength, and toughness with respect to N. Error bars indicate the standard deviation.

A. Stiffness

With the four geometries and three orders of hierarchy, stiffness increases over an order of magnitude, from the least stiff first-order anti-trapezoidal suture interface to the stiffest third-order triangular suture interface. For all values of N, the anti-trapezoidal geometry had the lowest stiffness, followed by the rectangular, trapezoidal, and triangular geometries with increasing stiffness. Increasing the order of hierarchy amplified the effect of geometry on stiffness. For $N = 1$, the stiffnesses were more similar to each other (ranging from 37 to 115 MPa), with the triangular geometry possessing a stiffness approximately three times that of the anti-trapezoidal geometry. With increasing N, the stiffness difference between the various geometries became more pronounced, ranging from 54 to 419 MPa and with the triangular geometry possessing a stiffness over six times that of the anti-trapezoidal geometry. Considering that the stiffness of an Nth hierarchical suture interfaces depends on the tensile and shear modulus of the $(N - 1)$th hierarchical suture interface,[20] a small difference in stiffness between two geometries at $N = 1$ can easily become significant at $N = 3$.

For all geometries except the anti-trapezoidal geometry, the stiffness was highest at $N = 3$, with the triangular geometry showing a stiffness three times greater than the first-order triangular suture interface. With an increased order of hierarchy, two opposing factors influenced the stiffness: the increased order of hierarchy resulted in a stiffness amplification due to an increased effective stiffness of the first-order interfaces, while maintaining a constant overall volume fraction resulted in a decreased stiffness due to the reduction of the building block (minor teeth) volume fraction.[20] For the rectangular, trapezoidal, and triangular geometry, the amplification from increasing the order of hierarchy was greater than the decrease from a reduction of building block volume fraction. However, for the anti-trapezoidal geometry, there was a peak at $N = 2$. The more significant effect from the lowering of building block volume fraction was due to the small cross-sectional area of the anti-trapezoidal geometry at the base of its teeth, and hence a decreased volume of tooth material under mechanical load.

B. Tensile strength

The tensile strength was taken to be the maximum stress that the suture interface undergoes under tension. When $N = 1$, all geometries exhibited similar strengths, the maximum strength was within 17% of the minimum strength; this strength then increased when $N = 2$ for the triangular and trapezoidal geometries and decreased for the rectangular and anti-trapezoidal geometries, resulting in a range of strengths of over 250% of the minimum strength. From $N = 2$ to $N = 3$, the strength of all geometries increased.

Depending on the failure mechanism, the strength corresponded to the stress at interfacial layer failure, tooth failure, or both simultaneously, whichever occurred first. Regardless of the failure mechanism leading to catastrophic failure, interfacial layer failure was observed to occur first in all samples. Therefore, the change in strength can be explained by the failure mechanisms of the interface, which are governed by the ratio of interfacial normal stress to interfacial shear stress. This effect was seen most clearly in the rectangular geometry. For $N = 1$ and at $N = 3$, the interfacial layer failed by shearing, while for $N = 2$, the interfacial layer failed due to normal stresses. Therefore, the strength of the first-order and third-order rectangular suture interfaces were higher than that of the

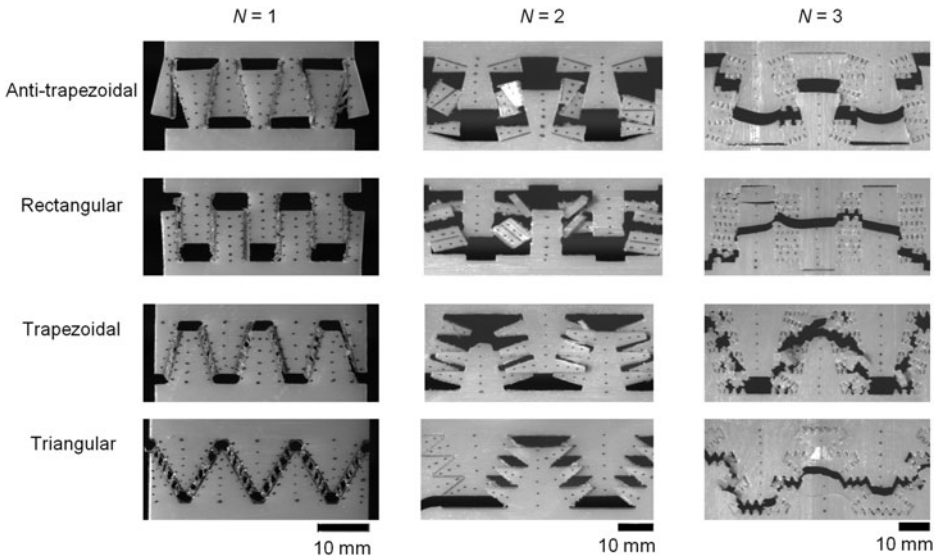

FIG. 3. Optical images of catastrophic failure of hierarchical suture interfaces under longitudinal tension.

second-order rectangular suture interfaces. Anti-trapezoidal suture interfaces followed a similar trend. On the other hand, there was no decrease in strength for trapezoidal and triangular geometries at $N = 2$. For these geometries, the larger cross-sectional area of the tooth base of the minor teeth provided for greater load bearing before the initial onset of failure.

C. Toughness

The influence of the order of hierarchy on tensile toughness (defined here as the total area under the stress–strain curve until complete failure) differed across geometries, with the triangular and trapezoidal exhibiting maximum toughness at $N = 3$, the rectangular at $N = 2$, and the anti-trapezoidal geometry at $N = 1$. For the anti-trapezoidal geometry, increasing N decreased the toughness, and it possessed the highest toughness relative to the other geometries at $N = 1$ due the interlocking of its teeth. This interlocking became less significant at higher N, since the failure of the minor and major teeth occurred before significant interlocking of the teeth. For the rectangular geometry, the toughness peaked at $N = 2$ with the other orders of hierarchy exhibiting similar toughnesses. At $N = 2$, the rectangular geometry required the failure of almost all of the minor teeth before catastrophic failure, greatly increasing the toughness. For both the trapezoidal and triangular geometry, the toughness increased with an increase in N, although the triangular geometry has a more significant increase in toughness with each increase in N. For the trapezoidal geometry, at $N = 2$, the suture interface was able to bear loads close to its maximum load-bearing capacity for some

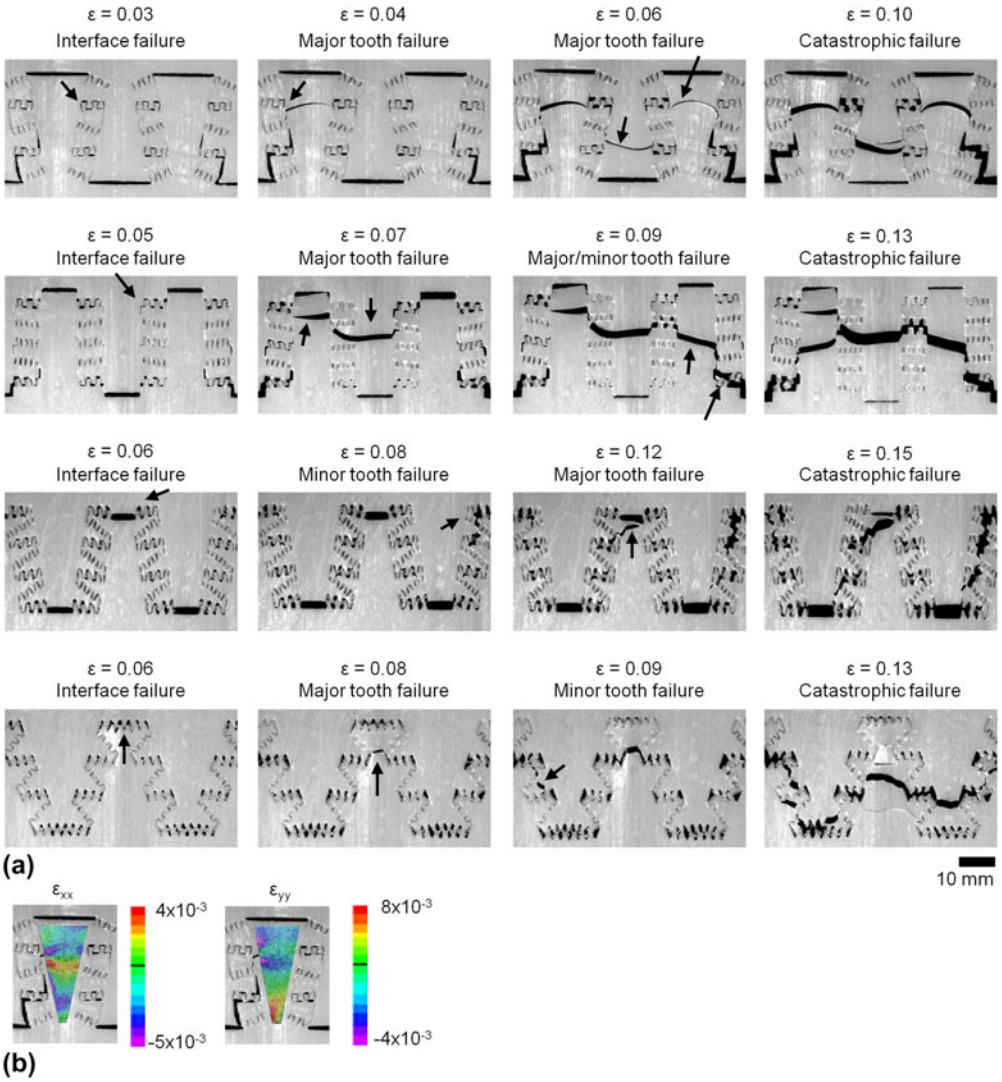

FIG. 4. Failure mechanisms of the third-order hierarchical suture interfaces. (a) Optical images of the third-order triangular and anti-trapezoidal suture interfaces, showing interface failure, minor and major tooth failure, and catastrophic failure, (b) strain contours of the third-order anti-trapezoidal suture interfaces immediately prior to major tooth failure.

strain before failing, as seen in the plateau of the stress–strain curve. For $N = 3$, graceful failure, a result of significant interfacial layer and minor teeth failure occurring before catastrophic failure, resulted in an increase in toughness. The triangular geometry exhibited an increased stiffness, strength, and strain at maximum load-bearing capacity, and graceful failure with an increased N that all contributed to its significant increase in toughness.

D. Failure mechanisms

As mentioned above, graceful failure is an important contribution to the increase in toughness of suture interfaces since the majority of the energy dissipation of hierarchical suture interfaces comes from post-failure mechanisms. As shown in Fig. 3, suture interfaces failed through major tooth failure, minor tooth failure, and interfacial layer failure. First-order suture interfaces failed mainly through interfacial layer failure. When $N = 2$, both interface failure and minor tooth failure occurred, with major tooth failure in the triangular geometry. For $N = 3$, interface failure, minor tooth failure, and major tooth failure all played a part in the failure mechanisms. While for $N = 1$, the anti-trapezoidal geometry is the only interlocking geometry, so for higher orders of hierarchy, interlocking is an inherent result of the geometry. As a result, the suture interfaces exhibited damage tolerance, where interface failure alone did not result in catastrophic failure.

The failure mechanisms of the third-order hierarchical suture interfaces were much more complex, as shown in Fig. 4(a), and determined the overall toughness of the suture interface. Catastrophic failure occurred when the cracks from major and minor teeth failure eventually coalesced to form a tortuous path across the suture interface. Therefore, the amount of interface failure and minor tooth failure prior to catastrophic failure greatly influenced the overall toughness of the interface. The major teeth of the anti-trapezoidal and rectangular geometries failed at lower strains of $\varepsilon = 0.04$ and 0.07, respectively, and therefore their load-bearing capacities fell quickly with each major tooth breakage. Triangular and trapezoidal geometries, on the other hand, exhibited significant interface and minor tooth failure prior to major tooth failure. In addition, even with initial minor tooth failure, the triangular and trapezoidal geometries were still able to maintain interlocking of the major teeth, exhibiting significant damage tolerance.

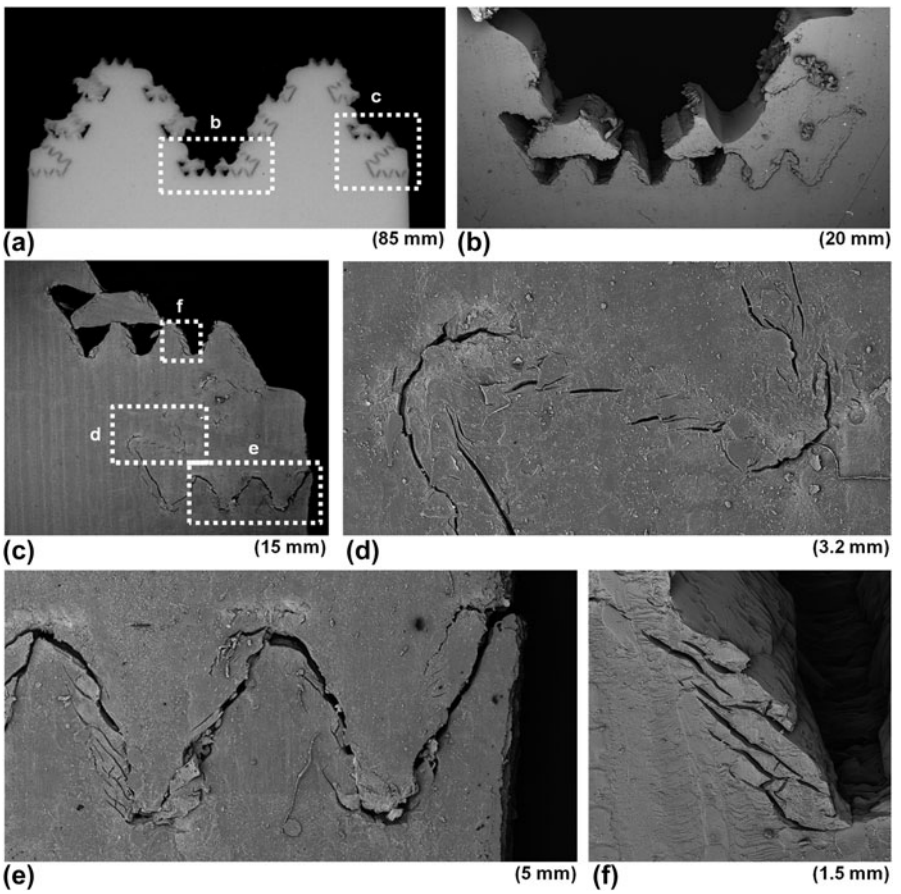

FIG. 5. Post-failure images, (a) optical, (b)–(f), scanning electron microscope images, of a triangular third-order hierarchical suture interface. Scales indicate the image width.

Tooth failure in first-order suture interfaces can occur for specific geometries, tip angles, and tooth to interfacial layer stiffness ratios, but always occurred at the base of the teeth. Third-order suture interfaces, on the other hand, exhibited major tooth failure near the middle or top of its teeth, even for anti-trapezoidal geometries, which had a small cross-sectional area at the base of its teeth. The location of major tooth failure can be explained by the strain contours shown in Fig. 4(b). The strain contours show the local strain in the anti-trapezoidal major tooth immediately prior to major tooth failure. Although the strain in the vertical direction is indeed greatest at the base of the tooth, there was a compressive strain from the interlocking of the teeth exactly where major tooth failure occurred. Failure along the middle of the major teeth allowed for interlocking even after tooth failure.

High resolution imaging of the third-order triangular suture interface specimen via SEM, post-failure, as shown in Fig. 5 revealed the deformation in the interfacial layer even in regions that remained intact. The failure of every interface in the triangular suture interface allowed for maximized energy dissipation. In addition,

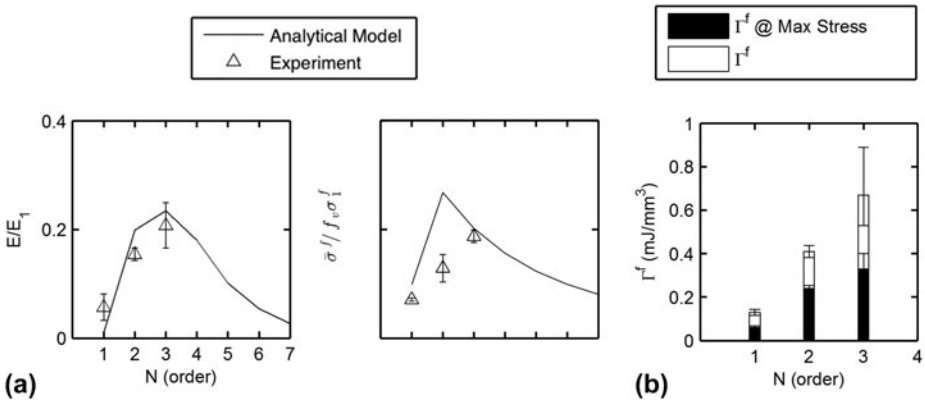

FIG. 6. Mechanical properties of triangular suture interfaces. (a) Experimental nondimensional stiffness and strength compared with predictions from the analytical model, (b) experimental toughness at maximum stress and total toughness. Error bars indicate the standard deviation.

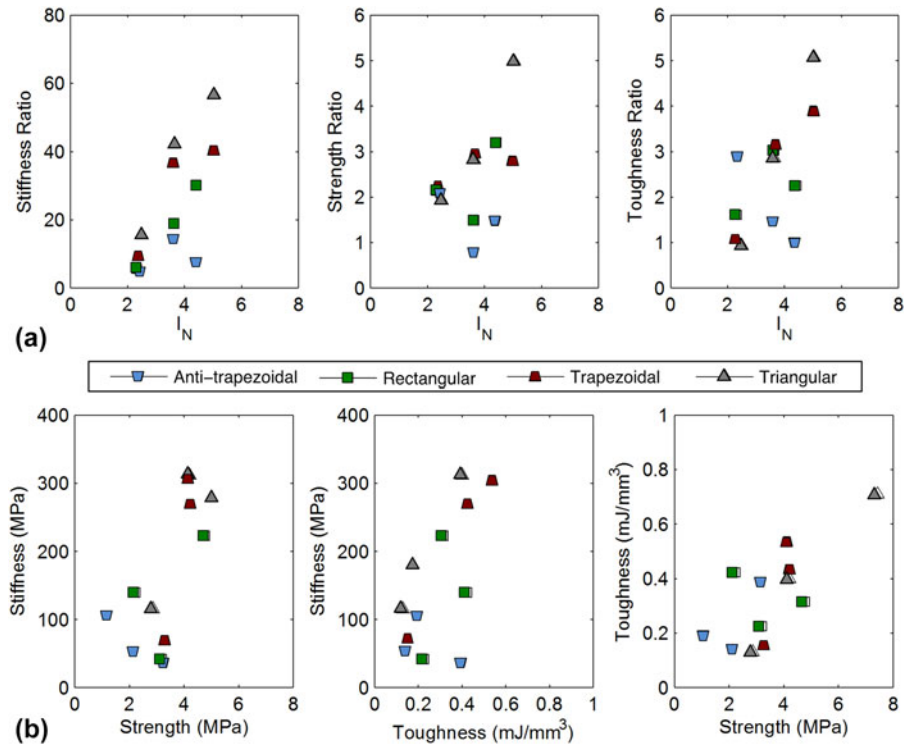

FIG. 7. Tunability and enhancement of mechanical properties of suture interfaces. (a) Experimental stiffness, strength, and toughness ratios of suture interfaces with respect to their suture complexity index, I_N, (b) stiffness versus strength, stiffness versus toughness, and toughness versus strength of hierarchical suture interfaces. Standard deviation of experimental values is given in Table I.

TABLE I. Experimental mechanical properties of hierarchical suture interfaces under longitudinal tension. Error is within one standard deviation of the mean.

N	Anti-trapezoidal	Rectangular	Trapezoidal	Triangular
		Stiffness (MPa)		
1	36.69 ± 2.52	41.80 ± 25.38	69.74 ± 25.38	115.30 ± 49.59
2	107.19 ± 23.23	139.90 ± 22.40	269.25 ± 21.34	311.79 ± 23.37
3	37.92 ± 53.89	187.66 ± 70.40	306.95 ± 37.49	419.48 ± 84.57
		Strength (MPa)		
1	3.19 ± 0.08	3.19 ± 0.16	3.35 ± 0.07	2.87 ± 0.11
2	1.17 ± 0.21	2.22 ± 0.24	4.29 ± 0.87	5.20 ± 1.02
3	2.17 ± 0.02	4.78 ± 0.03	4.20 ± 0.28	7.42 ± 0.47
		Toughness ($mJ/mm^3 \times 10^{-1}$)		
1	3.97 ± 0.20	2.24 ± 0.01	1.59 ± 0.21	1.31 ± 0.11
2	2.02 ± 0.12	4.22 ± 0.19	4.33 ± 0.60	4.03 ± 0.24
3	1.48 ± 0.41	3.40 ± 0.62	5.44 ± 0.76	7.14 ± 1.51

Figs. 5(d) and 5(f) show slanted cracks through the interfacial layer that correspond to the periodic cavitations observed in the interfacial layer. As opposed to the interfacial layer, which eventually failed through the stretching and shearing modes, resulting in rough surfaces, the failure of the teeth was more brittle and resulted in smooth surfaces, as seen in Fig. 5(b). In addition, layers through the thickness of the material in both the interfacial layer and teeth can be seen in the images of the tilted specimens in Figs. 5(b) and 5(d), that resulted from the intrinsic layer-by-layer fabrication method of additive manufacturing.

E. Comparison with analytical model

The analytical model presented in Li et al. (2012) predicted the stiffness, strength, and toughness of the first-, second-, and third-order triangular suture interfaces. Figure 6(a) shows a comparison between experimental results presented in this paper and the predicted mechanical properties. The model predicted the stiffness and strength of the triangular suture interfaces quite well with the exception of the strength of the second-order triangular suture interface. For this case, the experimental tensile strength is significantly less than the predicted. This can be explained by the effect of boundary conditions in the experiment, whether tooth failure occurs only at the edge, rather than across the entire suture interface.

As for toughness, it is difficult to capture this analytically due to the significant energy dissipation after maximum load-bearing capacity is exceeded. As shown in Fig. 6(b), triangular suture interfaces of all orders of hierarchy were able to dissipate energy significantly after reaching maximum load-bearing capacity. For all N, approximately 50% of the total toughness was due to the overall failure progression. Therefore, the difference in total toughness was doubled relative to the difference in toughness up to the peak stress when N was increased.

IV. DISCUSSION AND CONCLUSION

The stiffness, strength, toughness, and failure mechanisms of suture interfaces can be tailored or amplified by changing the order of hierarchy. An understanding of the underlying role of geometry and hierarchy in the mechanical behavior of suture interfaces will allow for the design of damage tolerant materials with tailored mechanical properties. In particular, the increase in hierarchy shows an enhancement or tunability of mechanical properties that can be utilized to diversify the current additive manufacturing materials library.

A. Enhancement and tunability of interface mechanical properties

Four suture interface geometries with three orders of hierarchy, each resulted in different combinations of stiffness, strength, and toughness. For a given tooth volume fraction, increasing the order of hierarchy increases the complexity of the design. This complexity can be quantified by a suture complexity index, I_N, which is defined by the total suture interfacial layer length over the horizontal length of the suture interface structure.[11] With this definition, a simple flat interface would have $I_N = 1$.

Figure 7(a) shows the stiffness, strength, and toughness ratios of geometric suture interfaces relative to a flat interface with respect to I_N. By increasing the suture complexity index by less than six times, the stiffness can be increased by 50 times, and strength and toughness increased by 5 times. Even doubling the suture complexity index can result in an order of magnitude increase in stiffness and double the strength for triangular suture interfaces. In addition, the increases in mechanical properties have a clear dependence on geometry, with the triangular and trapezoidal geometries resulting in the greatest increases generally, and the anti-trapezoidal geometry resulting in the least significant increase. With additive manufacturing, because added complexity and changes in geometry are easily accomplished, often with no net effect on total fabrication time, significant improvements in mechanical behavior of interfaces can be conveniently attained. Fine-tuning of mechanical properties can thus be easily accomplished through changes in suture interface geometry and complexity.

In addition, Fig. 7(b) shows that stiffness, strength, and toughness can all be improved without the usual tradeoff between the properties. For all three properties, triangular suture interfaces exhibit the highest stiffness, strength, and toughness. Apart from the triangular geometry, the general trend shows increased stiffness with increased strength and increased toughness for many designs. Therefore, the use of suture interface design in conjunction with additive manufacturing is a simple way of enhancing mechanical properties of interfaces.

B. Expanding the additive manufacturing materials library

Currently, a number of metallic, ceramic, and polymer materials can be utilized in additive manufacturing, but as in nature, the available materials and the mechanical behavior of the materials are limited compared with other manufacturing methods. Just as nature utilizes geometry to create materials with an incredible range of mechanical properties,[6,24,25] suture interfaces can also be utilized to expand the current range of mechanical properties available for additive manufacturing. As demonstrated by the results in this paper, bio-inspired hierarchical suture interface designs can enhance or tune mechanical properties of interfaces. Therefore, these same design principles can be utilized to combine currently available materials to create materials with different mechanical properties that can be easily fabricated via additive manufacturing.

C. Hierarchical suture interface designs with natural materials

In this manuscript, the influence of hierarchical suture designs with additively manufactured polymers was shown to amplify the toughness relative to flat interface designs. It is interesting to note that due to the inherently different mechanical properties of natural materials, the effect of soft hierarchical suture interface designs is expected to be even more largely amplified. As opposed to the ductile additively manufactured polymers used in the present study, many natural materials, such as the mineral phase of ammonite shells, aragonite, is brittle. With a brittle suture tooth material, hierarchical suture interface designs essentially provide the structure with increased ductility. In contrast, the hierarchical suture designs with organic interfacial layers reported in this present study are able to exhibit graceful failure, and as demonstrated, can greatly amplify the toughness of the synthetic structures relative to their natural biological counterparts.

ACKNOWLEDGMENTS

This research was supported (in part) by the U.S. Army Research Office under contract W911NF-13-D-0001. In addition, this research was conducted with Government support under and awarded by DoD, Air Force Office of Scientific Research, National Defense Science and Engineering Graduate (NDSEG) Fellowship, 32 CFR 168a.

REFERENCES

1. L. Wang, J. Lau, E.L. Thomas, and M.C. Boyce: Co-continuous composite materials for stiffness, strength, and energy dissipation. *Adv. Mater.* **23**(13), 1524 (2011).
2. A. Browning, C. Ortiz, and M.C. Boyce: Mechanics of composite elasmoid fish scale assemblies and their bioinspired analogues. *J. Mech. Behav. Biomed. Mater.* **19**, 75 (2013).
3. Y. Li, N. Kaynia, S. Rudykh, and M.C. Boyce: Wrinkling of interfacial layers in stratified composites. *Adv. Eng. Mater.* **15**(10), 921 (2013).
4. L.S. Dimas, G.H. Bratzel, I. Eylon, and M.J. Buehler: Tough composites inspired by mineralized natural materials: Computation, 3D printing, and testing. *Adv. Funct. Mater.* **23**(36), 4629 (2013).
5. S.A. Wainwright, W.D. Biggs, J.D. Currey, and J.M. Gosline: *Mechanical Design in Organisms* (Princeton Univ. Press, Princeton, NJ, 1976).
6. M.A. Meyers, P.Y. Chen, A.Y.M. Lin, and Y. Seki: Biological materials: Structure and mechanical properties. *Prog. Mater. Sci.* **53**(1), 1 (2008).
7. J.W.C. Dunlop, R. Weinkamer, and P. Fratzl: Artful interfaces within biological materials. *Mater. Today* **14**(3), 70 (2011).
8. H. Zhou and Y. Zhang: Hierarchical chain model of spider capture silk elasticity. *Phys. Rev. Lett.* **94**, 028104 (2005).
9. H. Yao and H.J. Gao: Mechanics of robust and releasable adhesion in biology: Bottom-up designed hierarchical structures of gecko. *J. Mech. Phys. Solids* **54**(6), 1120 (2006).
10. C.A. Long and J.E. Long: Fractal dimensions of cranial sutures and waveforms. *Acta Anat.* **145**(3), 201 (1992).
11. W.B. Saunders: Evolution of complexity in paleozoic ammonoid sutures. *Science* **286**(5440), 760 (1999).
12. C.R. Jaslow: Mechanical properties of cranial sutures. *J. Biomech.* **23**(4), 313 (1990).
13. C.R. Jaslow and A.A. Biewener: Strain patterns in the horncores, cranial bones and sutures of goats (Capra hircus) during impact loading. *J. Zool.* **235**(2), 193 (1995).
14. E.G. Allen: Understanding ammonoid sutures. *Cephalopods Present and Past: New Insights and Fresh Perspectives*, 159, 2007.
15. S. Krauss, E. Monsonego-Ornan, E. Zelzer, P. Fratzl, and R. Shahar 2009: Mechanical function of a complex three-dimensional suture joining the bony elements in the shell of the red-eared slider turtle. *Adv. Mater.* **21**(4), 407 (2009).
16. Z. Sun, E. Lee, and S.W. Herring: Cranial sutures and bones: Growth and fusion in relation to masticatory strain. *Anat. Rec., Part A* **276**(2), 150 (2004).
17. Y. Li, C. Ortiz, and M.C. Boyce: Stiffness and strength of suture joints in nature. *Phys. Rev. E* **84**, 062904 (2011).
18. J. Song, S. Reichert, I. Kallai, D. Gazit, M. Wund, M.C. Boyce, and C. Ortiz: Quantitative microstructural studies of the armor of the marine threespine stickleback (Gasterosteus aculeatus). *J. Struct. Biol.* **171**(3), 318 (2010).
19. W.B. Saunders and D.M. Work: Shell morphology and suture complexity in upper carboniferous ammonoids. *Paleobiology* **22**(2), 189 (1996).
20. Y. Li, C. Ortiz, and M.C. Boyce: Bioinspired, mechanical, deterministic fractal model for hierarchical suture joints. *Phys. Rev. E* **85**, 031901 (2012).
21. T.L. Daniel, B.S. Helmuth, W.B. Saunders, and P.D. Ward: Septal complexity in ammonoid cephalopods increased mechanical risk and limited depth. *Paleobiology* **23**(4), 470 (1997).
22. M.A. Hassan, G.E.G. Westermann, R.A. Hewitt, and M.A. Dokainish: Finite-element analysis of simulated ammonoid septa (extinct Cephalopoda): Septal and sutural complexities do not reduce strength. *Paleobiology* **28**(1), 113 (2002).
23. Y. Li, C. Ortiz, and M.C. Boyce: A generalized mechanical model for suture interfaces of arbitrary geometry. *J. Mech. Phys. Solids* **61**(4), 1144 (2013).
24. J.W.C. Dunlop and P. Fratzl: Biological composites. *Annu. Rev. Mater. Res.* **40**, 1 (2010).
25. C. Ortiz and M.C. Boyce: Bioinspired structural materials. *Science* **319**(5866), 1053 (2008).